PREPRINT UCRL- 79775

CONF-771136--20

Lawrence Livermore Laboratory

2660 Å HOLOGRAPHIC INTERFEROMETRY OF LASER PRODUCED PLASMAS FROM TILTED DISK TARGETS

MASTER

J. M. Auerbach, D. T. Attwood, P. H. Y. Lee and D. W. Sweeney

October 21, 1977

This paper was prepared for submission to the APS Plasma Physics Meeting of the American Physical Society, Atlantic, Georgia, November 5-11, 1977.

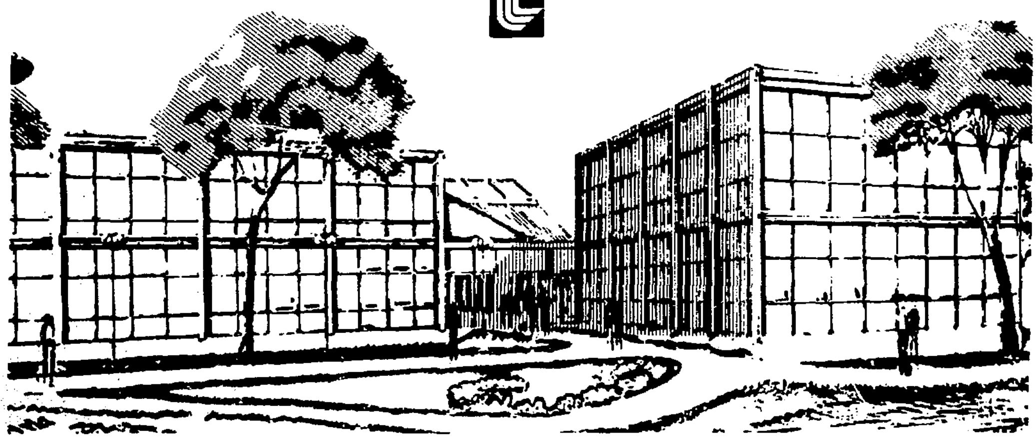

Abstract Submitted

for the APS Plasma Physics Meeting of the

American Physical Society

November 5-11, 1977

Physics and Astronomy
Classification Scheme
Number 52

Bulletin Subject Heading in
which Paper should be placed
2.1.4 Pellet Experiments

2660Å Holographic Interferometry of Laser Produced Plasma from Tilted Disk Targets. Jerome M. Auerbach, David T. Attwood, Peter H. Y. Lee and Donald W. Sweeney, Lawrence Livermore Laboratory.**--Using double exposure holographic interferometry, an investigation has been made of the Nd laser produced plasmas surrounding disk targets irradiated at different angles of incidence. Measurements have produced a detailed description of the plasma profile necessary for realistic simulations of resonance absorption. A 2660Å 15 psec probe pulse is produced by frequency quadrupling a fraction of the main Nd laser pulse from the Janus laser. F/1 and f/10 lenses were utilized to irradiate the targets with intensities ranging from 10^{13} w/cm^2 to 10^{16} w/cm^2. Measurements have produced the shape of the electron density profile near critical, the direction of the plasma blowoff, and revealed transverse rippling of the isodensity surfaces.

**Supported by U. S. ERDA Contract W-7405-ENG-48

Submitted by

Jerome M. Auerbach
University of California
Lawrence Livermore Laboratory
P. O. Box 808, L-549
Livermore, CA 94550

(10 minute paper) ORAL
To proceed paper by
D. T. Attwood et al,
"Profile Steepening,
Cavity Formation, and
Crtical Surface
Rippling in Nd-Laser
Produced Plasmas."

2660 Å Holographic Interferometry of Laser Produced Plasmas from Tilted Disk Targets

A detailed description of the plasma region between the intense laser light field and the thermonuclear fuel is essential in design of the most efficient schemes for laser fusion. The nature of the plasma profile determines the efficiency of laser light absorption. For large gradient scale lengths and transverse extents, Brillouin backscatter[1-3] can seriously degrade absorption at high laser intensities. At the other extreme, short gradient scale lengths determine the dominance of resonance absorption[4-6] over other absorption processes. Simulations of resonant absorption require accurate estimates of both direction and magnitude of the density gradient to check on the accuracy of the simulation of profile modification when pondermotive forces approach the plasma pressure $V_{os}/V_e \rightarrow 1$. Resonance absorption also being polarization and incidence angle dependent is influenced by ripples, cavities and waviness in the isodensity surfaces of the plasma. Numerical simulations[7] have shown that ripples, bubbles and cavities can develop near the critical density surface when intensity variations exist in the incident laser pulse. An important input to these simulations would be an experimental observation of the fluctuations in the isodensity surfaces of an irradiated target. Isodensity surface waviness has been used by Thomson, et al,[8] to interpret recent angle and polarization dependent absorption experiments made by Manes, et al.[9]

Motivated by the need for a detailed spatial description of the plasma, a holographic interferometry system was developed at Lawrence Livermore Laboratory to probe the plasma of Nd laser irradiated targets with a spatial resolution of 1 μm and a temporal resolution of 15 psec. Double exposure holographic interferometers have several advantages over conventional interferometers such as the Mach-Zehnder.[10]

The primary advantages in this application[11] are the ability to provide simple and accurate focusing to one micron accuracy and to allow the use of coherent imaging techniques to greatly reduce the obscuring effects of plasma harmonic light emission at the same frequency. In addition, since the two beams of the interferometer follow essentially the same path, the effects of distortion in optical windows are not as severe as in interferometers with separate beam paths.

To provide probing of the plasma to densities beyond the critical value for 1.06 μm light, a frequency quadrupled scheme was used.[12] Figure 1 shows the maximum probing depth for the second and fourth harmonics of 1.06 μm light in a spherical plasma distribution typical of laser fusion targets. Figure 1 shows that 4ω light can reach four times the density as 2ω light. The information to be gained far outweighs the difficulties in using UV optics. Frequency quadrupling of a portion of the heating pulse for a probe pulse allows precise and stable synchronization of the two pulses. Probing at different times to within a few picoseconds can be accomplished with simple optical delay lines. The frequency quadrupled probe pulse optics setup, as incorporated into the JANUS laser facility, is shown in Figure 2. 50% of the energy of the oscillator pulse (30 psec FWHM) is used in the probe beam optics. The remainder is amplified to give a single beam irradiation energy from 0.1J - 6J. The 1.06 μm pulse in the probe optics is first amplified by a YAG preamp to bring the intensity up to the level required for significant energy conversion in the nonlinear crystals. Energy conversion is limited to less than 10% per crystal to maximize pulse shortening.[12] The pulse is smoothed with a 300 μm pinhole spatial filter and apodized aperture to give it a "super gaussian" spatial profile. After reducing the beam to the proper extent for the conversion crystals, IR to green conversion is done in a KDP crystal and then green to UV conversion is done in an ADP crystal. With the JANUS oscillator in short pulse operation, the UV probe pulse after the ADP crystal has on the average, a FWHM of 15 psec and an energy of 3 μJ. Timing of the arrival of the probe pulse on target with respect to the arrival of the heating pulse is accomplished using an optical delay setup made of fused silica prisms as shown in the figure. Initial sychronization of the two pulses was accomplsihed to 10 psec accuracy with ultrafast streak photography.

The interferometer setup for the JANUS target chamber is illustrated in Figure 3. The object and reference beams are split outside the target chamber in an intensity ratio of 1:10. Path length matching to within the coherence length of the pulse (500 μm) is done with a precision mirror mount. The object beam is collimated before traversing the target plasma and then passes through a 10 x, 0.2 NA microscope objective. The reference beam passes through a 4 cm focal length lens to provide a convenient size beam area at the film plane.

Forty micron diameter glass microspheres and 50 μm, 70 μm, 170 μm, and 340 μm diameter glass and parylene disks were irradiated with 0.1 - 5J, 30 psec FWHM laser pulses at the focus of either an f/10 or f/1 lens. The f/10 lens provided a planar intensity front in the range of 10^{13} - 10^{15} w/cm^2. This was used to study the plasma region of tilted disk targets. The f/1 lens allowed use of small focal spots giving intensities on target in excess of 10^{16} w/cm^2. Details of the microsphere experiments will be discussed in the next paper, while the disk results will form the subject of this paper. Figure 4 summarizes the results of the experiments.

The experiments on 170 μm diameter parylene disk targets tilted with respect to the beam axis provided crucial information for modeling angular dependent absorption. Figure 5 shows the interferogram of a 45° tilted parylene disk before irradiation and at the peak of the heating pulse. The second photograph indicates that the large-scale blowoff direction is perpendicular to the initial target surface. The presence of ripples in the fringe pattern suggests that on a smaller scale, the incident light sees locally deformed isodensity surfaces. This gives validity to the analysis of Thomson, et al,[8] that waviness in the critical surface tends to smear out the sharp resonance absorption curve predicted by Estabrook, et al[5], for a plane wave incident on a flat plasma.

Interferometry reveals enlightening details on each target shot. For example, Figure 6 shows a disk tilted at 22° in which there was formation of a depression and breakthrough at the peak of the pulse. Another interesting effect that was observed was prepulse damage. This is illustrated in Figure 7.

Several factors influence the quality of the interferograms. Excessive refraction of probe rays in high density regions lead to loss of these rays at the imaging optics. Harmonic light emission at high intensities on target will completely obscure fringes. High blowoff velocity can lead to fringe smearing. These effects will be discussed in more detail later, but it suffices to say at this point that these factors prevented obtaining, to date, interferograms of disks with complete fringe information up to critical density, other than for low intensity shots, i.e., $I \leq 10^{14}$ s/cm^2. Figure 7 shows an excellent interferogram of a disk target normal to the beam axis irradiated at an intensity of ~ 10^{13} w/cm^2. Abel Inversion of the interferogram[13] yielded the axial profile shown on the right of the figure. The probe rays reached critical density (10^{21} cm^{-3}). The smooth profile shows no modification due to radiation pressure effects.

In addition to the axial density profile at low intensities, the disk interferograms provided a detailed description of the formation of cavities or depressions in the plasma at high intensities. In Figure 8, one sees an interferogram of a 70 μm disk irradiated at an intensity of 3 x 10^{14} w/cm^2. The flat fringes in the subcritical region correspond to a depression in the isodensity surfaces as the Abel Inversion for a level 16 μm above the initial target surface indicates. For comparison, the interferogram of Figure 7 with an accompanying radial density profile is shown. The profile shows no depression. The two results demonstrate the correlation between higher intensity and the formation of a cavity in the plasma.

As described above, most of the disk experiments failed to provide density information near the critical value. The cause was the loss of fringes corresponding to rays that had probed through the high density region of the plasma. Refraction losses play a dominant role in this area.

The angle of refraction Θ of a ray through the plasma depends on the following factors:

$$\Theta \sim \frac{nL}{\ell}$$

n is the mean density traversed.

L is the path length of the ray through the plasma.

ℓ is the axial gradient scale length of the plasma.

For large Θ the rays miss the aperture of the collecting optics. The objective is to probe plasmas to as large a value of n as possible; therefore, for fixed Θ, one must minimize L, i.e., use the smallest targets possible. This step was made by using 50 μm - 70 μm acrylic disks. These targets were probed during irradiations at intensities of 10^{14} - 10^{15} w/cm^2. A typical interferogram of these small targets is shown in Figure 9. Unexpectedly, fringe information in the high density region of the plasma was completely lost. This loss of fringes is attributed to high blowoff velocities. An elementary analysis will show that fringe smearing varies as the following product

$$\text{f.s.} \sim \frac{vn}{\ell} L\tau$$

where v is the plasma blowoff velocity and τ is the probe pulse duration. For L and τ fixed, one sees that a high velocity and density gradient will lead to fringe smearing. Hence, one must conclude that with the high intensity shots with a small value of L, blowoff velocity was of such magnitude as to cause significant fringe smearing. Thus, probing to densities in excess of n_c was not possible with disk targets irradiated with $I \gtrsim 10^{15}$ w/cm^2. Information obtainable is only the shape of the subcritical region. The solution to this problem is to use a target geometry which will give:

(1) a lower value of L.

(2) a lower value of v.

Utilizing small ($\sim$ 40 μm diameter) glass microshells appears to be a solution. These experiments which will be described in the next paper.

In conclusion, holographic interferometry of disk targets have revealed the nature of the plasma profile and provided valuable data for interpretation of resonance absorption experiments. Figure 11 shows the modifications to plane surface simulations that must be made.

The authors acknowledge the excellent technical assistance of E. L. Pierce and for helpful discussions with H. Ahlstrom, W. Mead, E. Storm, and C. Max.

References

1. W. L. Kruer, E. J. Valeo, and K. G. Estabrook, "Limitation of Brillouin Scattering in Plasmas", Phys. Rev. Lett. 35, 1076 (1975).

2. D. W. Forslund, J. M. Kindel, E. L. Lindman, "Plasma Simulation Studies of Stimulated Scattering Processes in Laser Irradiated Plasmas", Phys. of Fluids, 18, 1017 (1975)

3. D. W. Phillion, W. L. Kruer, V. C. Rupert, LLL UCRL-79769, September 1977.

4. D. W. Phillion, R. A. Lerche, V. C. Rupert, R. A. Haas, M. J. Boyle, LLL UCRL-78444, June 1977 (submitted to Phys. of Fluids).

5. K. G. Estabrook, E. J. Valeo, W. L. Kruer, Phys. of Fluids 18, 1151 (1975).

6. K. G. Estabrook, E. J. Valeo, W. L. Kruer, Phys. Lett. 49A, 109, 1974.

7. K. Estabrook, Phys. of Fluids, 19, 1733, (1976).

8. J. J. Thomson, W. L. Kruer, A. B. Langdon, C. E. Max, W. C. Mead, LLL UCRL 78444 (Rev. I) (submitted to Appl. Phys. Lett.)

9. K. R. Manes, V. C. Rupert, J. M. Auerbach, P. Lee, and J. E. Swain, Phys. Rev. Lett. 39, 281 (1977)

10. R. J. Collier, C. B. Burckhardt, L. H. Lin, Optical Holography, New York, Academic Press, 1971.

11. D. T. Attwood, L. W. Coleman and D. W. Sweeney, Appl. Phys. Lett. 26, 616 (1975); D. T. Attwood Proc. XII Int'l. Congress on High Speed Photography, Toronto, Canada (1976), LLL UCRL-77744.

12. D. N. Nikogosyan, Sov. J. Quant, Electron 7, 1 (1977); D. T. Attwood, E. L. Pierce, and L. W. colemen, Optics Commun. 15, 10 (1975).

13. D. W. Sweeney, D. T. Attwood, L. W. Coleman, Appl. Optics 15, 1126 (1976)

List of Figures

REFRACTION OF AN OPTICAL PROBING PULSE

$$\tan \theta_c \simeq 0.31 \frac{L}{\ell}\left(\frac{\lambda_p}{\lambda_h}\right)^2$$

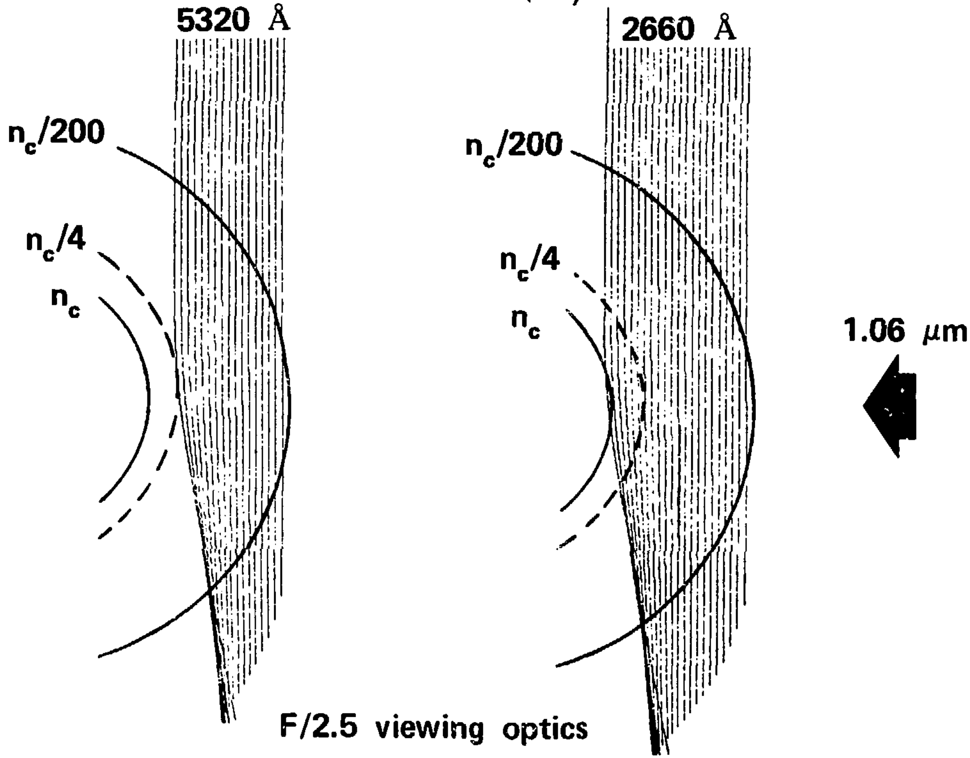

$$\frac{n}{n_c} = e^{-r/\ell}$$

$n_c = 10^{21}$ e/cc

$\ell = 15\ \mu m$

Figure 1

UV HOLOGRAPHIC INTERFEROMETER PROBE PULSE OPTICS

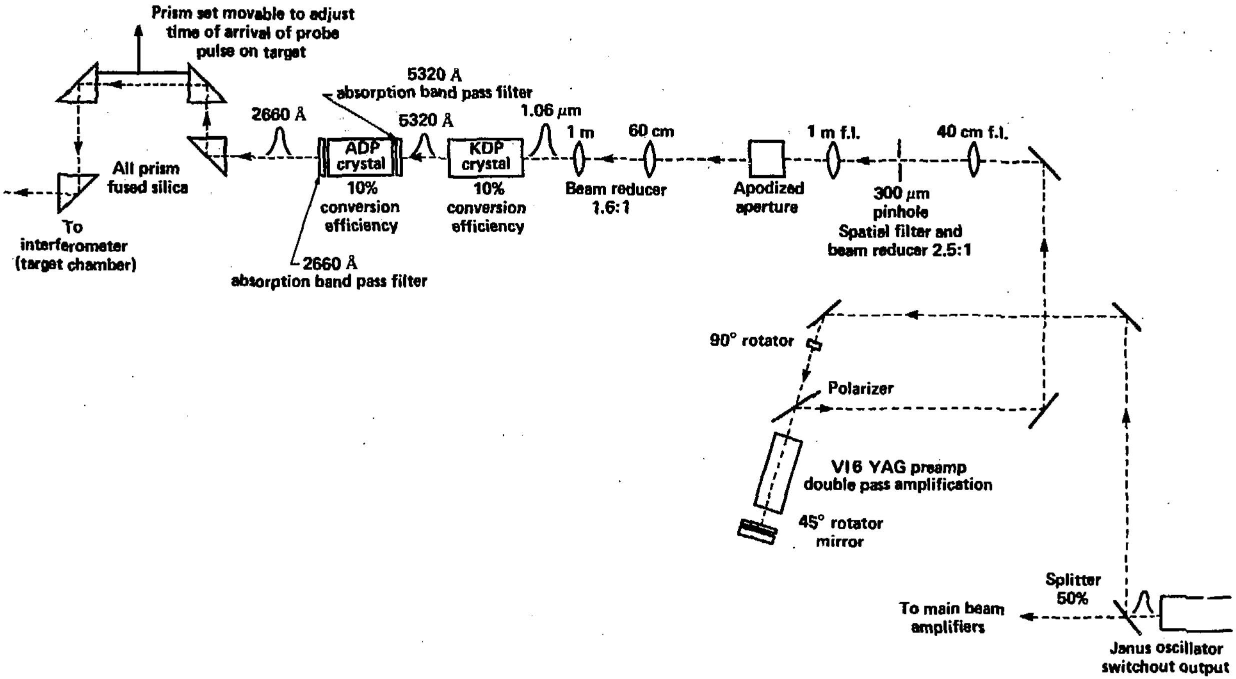

20-01-0877-1521

Figure 2

UV HOLOGRAPHIC INTERFEROMETER TARGET CHAMBER SETUP

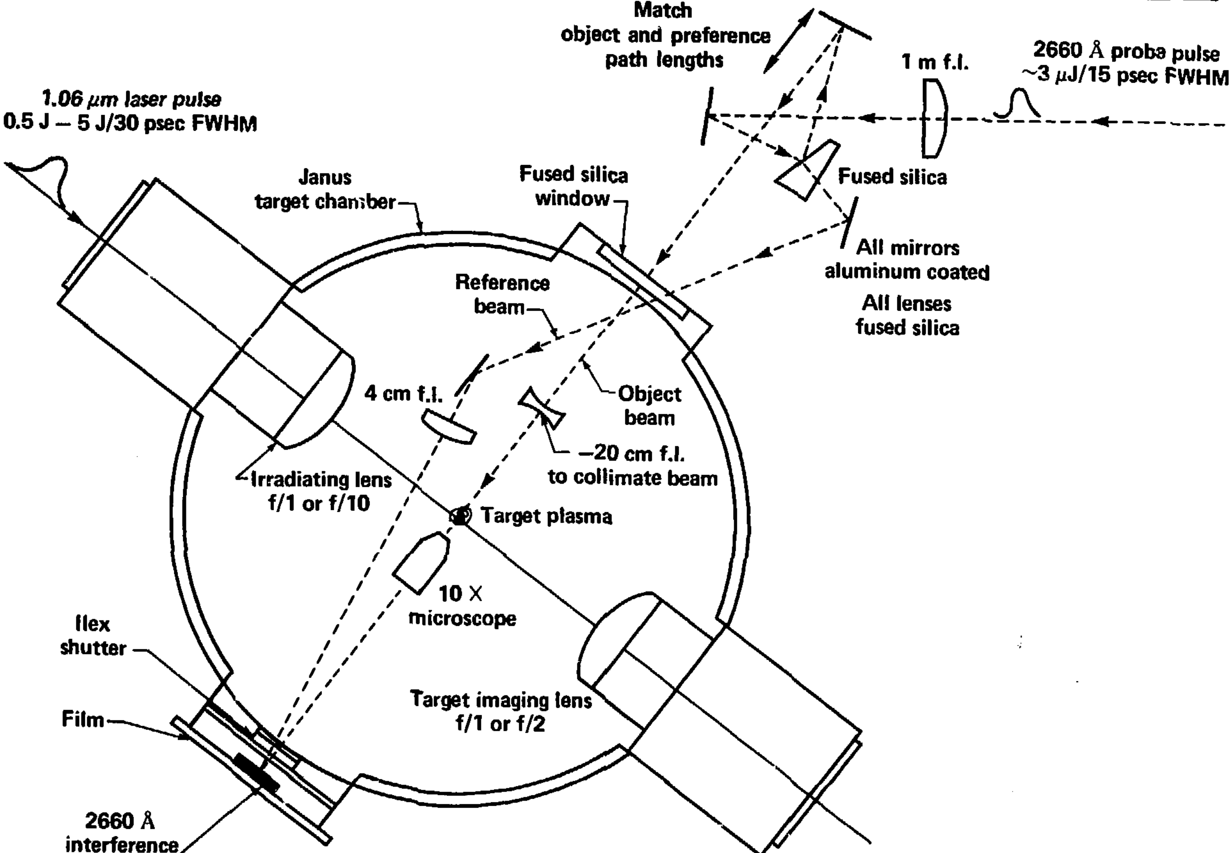

20-01-0877-1520

Figure 3

DISK INTERFEROMETRY EXPERIMENTS – RESULTS

Direction of the plasma blowoff
Waviness and cavities of isodensity surfaces
Axial density profile for low intensities ($\lesssim 10^{14}$ W/cm^2).

Limiting factors at high intensities ($> 10^{15}$ W/cm^2)
Smearing of fringes due to high velocity refraction
Loss of fringes in high density regions.

Obscuration of fringes by very strong emission of 2W and 4W harmonic light from plasma for $I \geqslant 5 \times 10^{15}$ W/cm^2.
Effects can be reduced by defocusing techniques.

20-90-1077-2129

Figure 4

PLASMA BLOWOFF OF A TILTED TARGET IS NORMAL TO THE INITIAL SURFACE

Target before irradiation

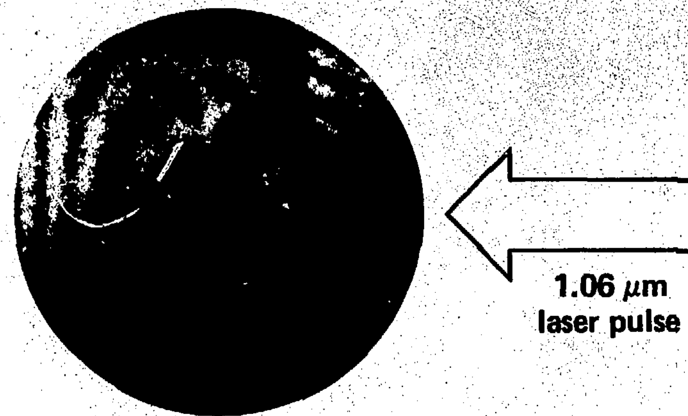

Shot: 77072604
Target: 175 μm parylene disk
tilt = 45°
Intensity on target: 3.5×10^{15} W/cm^2
Probe time: peak of main pulse

20-90-1077-2130

Figure 5

DETAILED DESCRIPTION OF EACH IRRADIATED TARGET

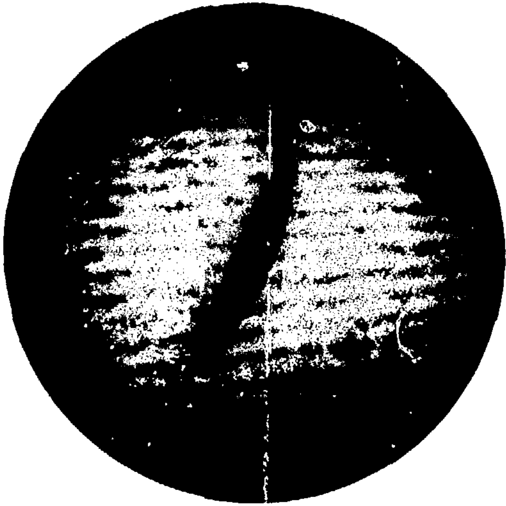

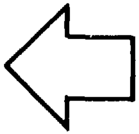

Target tilted 21° to beam axis

Shot: 77071403

Target: 180 μm dia parylene disk

Intensity on target : 7.3×10^{15} W/cm^2

Probe time : peak of heating pulse

Early breakthrough of plasma at rear of target

20-90-1077-2200

DISK INTERFEROGRAM AND AXIAL DENSITY PROFILE

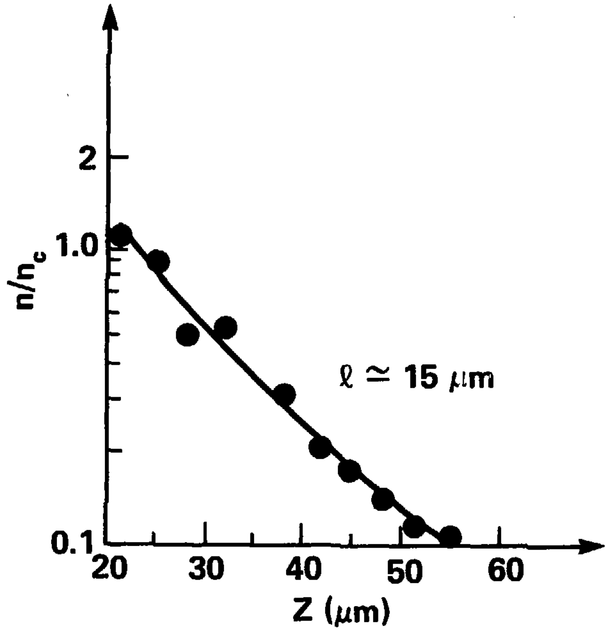

Shot: 77070706
Target: 170 μm dia parylene disk
Intensity on target: 3×10^{13} W/cm^2

Axial density profile along centerline
Probe time: peak of laser heating pulse
$n_c = 10^{21}$ cm^{-3}
Z height above intial target surface

20-90-1077-2201

DENSITY PROFILE INDICATES PRESENCE OF CAVITY

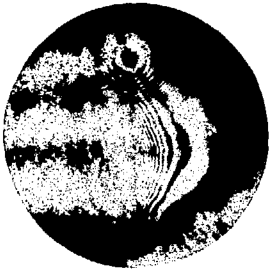

Shot: 77070706
Target: 170 μm dia parylene disk
Intensity on target: 3×10^{13} W/cm^2

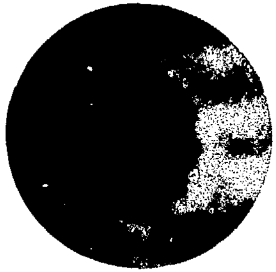

Shot: 77051205
Target: 70 μm dia glass disk
Intensity on target: 3×10^{14} W/cm^2

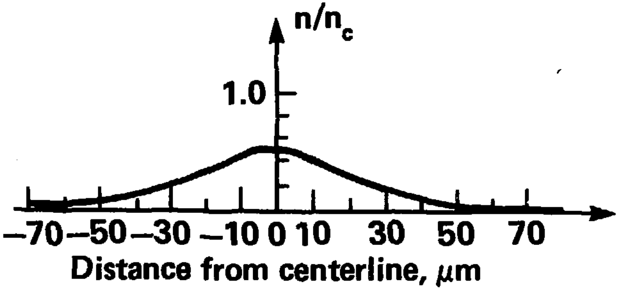

Radial density profile 9 μm above initial target surface

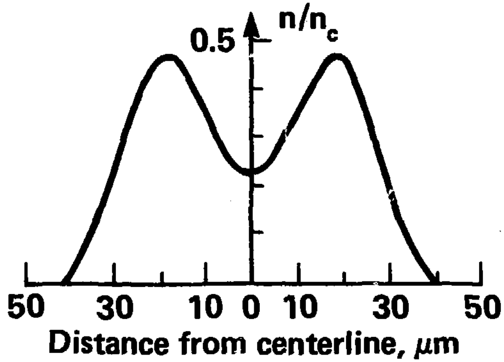

Radial density profile 12 μm above initial target surface

20-90-1077-2199

BLOWOFF VELOCITY IS A LIMITING FACTOR IN INTERFEROMETRY OF DISK TARGETS

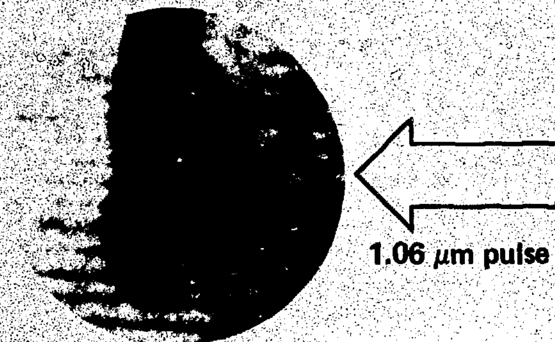

Refraction loss

$\theta \sim \nabla n_z L$

Fringe smearing

$\nabla n_z V \tau L \sim \lambda/2$

$\nabla n_z \sim \frac{n}{L}$

Shot: 77072802
Target: 56 μm dia disk
Intensity on target: 1.8×10^{15} W/cm^2
Probe time: peak of main pulse

20-90-1077-2128

Figure 10

IMPACT ON ANGLE DEPENDENT ABSORPTION STUDIES:

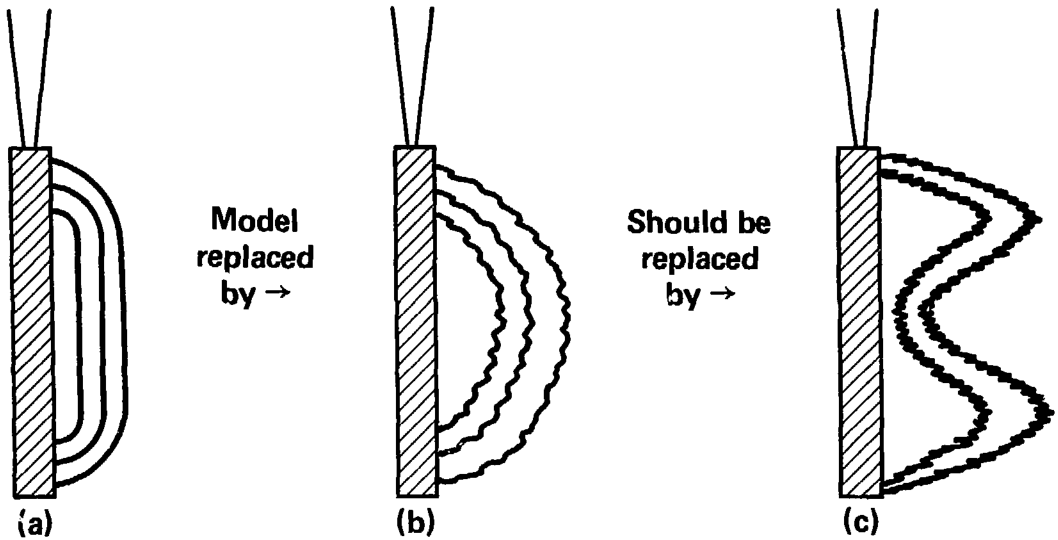

20-01-1077-2272

Figure 11